Procaine effects on single sarcoplasmic reticulum Ca^{2+} release channels

Alexandra Zahradníková and Philip Palade
Department of Physiology and Biophysics, The University of Texas Medical Branch, Galveston, Texas 77555 USA; and
Institute of Molecular Physiology and Genetics, Slovak Academy of Sciences, Bratislava, Slovakia

ABSTRACT The effects of the Ca^{2+}-induced Ca^{2+} release blocker procaine on individual sarcoplasmic reticulum Ca^{2+} release channels have been examined in planar lipid bilayers. Procaine did not reduce the single channel conductance nor appreciably shorten the mean open times of the channel; rather, it increased the longest closed time. These results indicated that procaine interacted selectively with a closed state of the channel rather than with an open state. Gating of the sarcoplasmic reticulum Ca^{2+} release channel was described by a modified scheme of Ashley and Williams (1990. *J. Gen. Physiol.* 95:981–1005), including an additional long-lived closed state. Computer simulations determined that procaine was more likely to interact with this long-lived Ca^{2+}-bound closed state of the channel rather than with other states of the channel. Simulations with the same model were also able to reproduce a prominent Ca^{2+}-sensitive transition between "random" and "bursting" forms of gating of the channel, variations of which may account for "gearshift" behavior reported in studies with this and other single channels.

INTRODUCTION

The identity of the sarcoplasmic reticulum calcium release channel (1), also called the ryanodine receptor (2), as the physiological Ca^{2+} release pathway has been inferred from structural (3) as well as pharmacological (4–6) evidence. Although numerous studies have focused on the effects of many agonists on this channel at the single channel level (7–14), there are few reports focusing on the mode of action of Ca^{2+} release channel antagonists (15). A number of additional reports mention effects of certain antagonists (e.g., 1, 11, 16–18), but, with the possible exceptions of Mg^{2+} and calmodulin, no antagonist extensively used in physiological experiments has been studied in detail at the single channel level.

Although the main physiological effects of procaine and other local anesthetics are those exerted at low concentrations on sodium channels, thus exerting a local anesthetic effect on nerves (19) and antiarrhythmic actions on the heart (20), it has been used widely as a research tool to study calcium release in muscle due to the inhibitory action that it exerts on sarcoplasmic reticulum Ca^{2+} release channels. Procaine was one of the first agents to be identified as an inhibitor of caffeine- and Ca^{2+}-induced Ca^{2+} release from the sarcoplasmic reticulum (21, 22). Its effects have been noted in skeletal muscle fiber experiments on vertebrates (23–25) as well as invertebrates (26, 27) and in skinned fiber studies of Ca^{2+} release (28, 29) as well as in studies on isolated sarcoplasmic reticulum (22, 30–32). Its actions on excitation–contraction coupling in cardiac muscle also appear to involve the block of Ca^{2+}-induced Ca^{2+} release (33–36).

Despite the widespread usage of procaine as an inhibitor of Ca^{2+} release, very little is known about its mechanism of action on the Ca^{2+} release channel of the sarcoplasmic reticulum. Incorporation of the Ca^{2+} release channel into planar lipid bilayers (37) affords an opportunity to examine the dynamics of the blockade exerted by procaine on this channel.

Because we anticipated that the blocking action of procaine might involve rapid, difficult to resolve closures, we elected to work with cardiac sarcoplasmic reticulum Ca^{2+} release channels (10–12, 38) rather than with their skeletal muscle counterparts, whose mean open times under most circumstances are more difficult to fully resolve within the bandwidth limitations of most recording systems. Although there are some quantitative differences in the sensitivity of cardiac and skeletal release channels toward certain agents (39), the qualitative effects of most substances are the same on both channels (18).

MATERIALS AND METHODS

General methods

Canine cardiac microsomes were prepared by a minor modification of the procedures of Harigaya and Schwartz (40). Briefly, canine hearts were removed under pentobarbital anesthesia, rinsed with chilled 0.9% NaCl, 10 mM tris(hydroxymethyl)-aminomethane Maleate, pH 7.3, and the ventricles cleaned of large vessels and connective tissue. The ventricles were then minced in a small precooled food processor before Polytron homogenization (probe MPT-20; Brinkmann Instruments, Inc., Westbury, NY) in 40-g batches with 3 vol of the above saline. Homogenization was carried out as three 15-s bursts separated by >30-s rest intervals on ice. The resultant homogenate was then centrifuged at 4,000 *g* for 20 min to remove cellular debris and nuclei and then recentrifuged successively at 8,000 *g* for 20 min and 40,000 *g* for 30 min to obtain two crude microsomal membrane fractions that were resuspended in the above saline supplemented with 10% sucrose and

The experimental part of this work was performed during the postdoctoral stay of A. Zahradníková in the Department of Physiology and Biophysics, The University of Texas Medical Branch, Galveston, TX 77555.

Address correspondence to Dr. Philip Palade, Department of Physiology and Biophysics, Basic Science Building (Route F-41), The University of Texas Medical Branch, Galveston, TX 77555, USA.

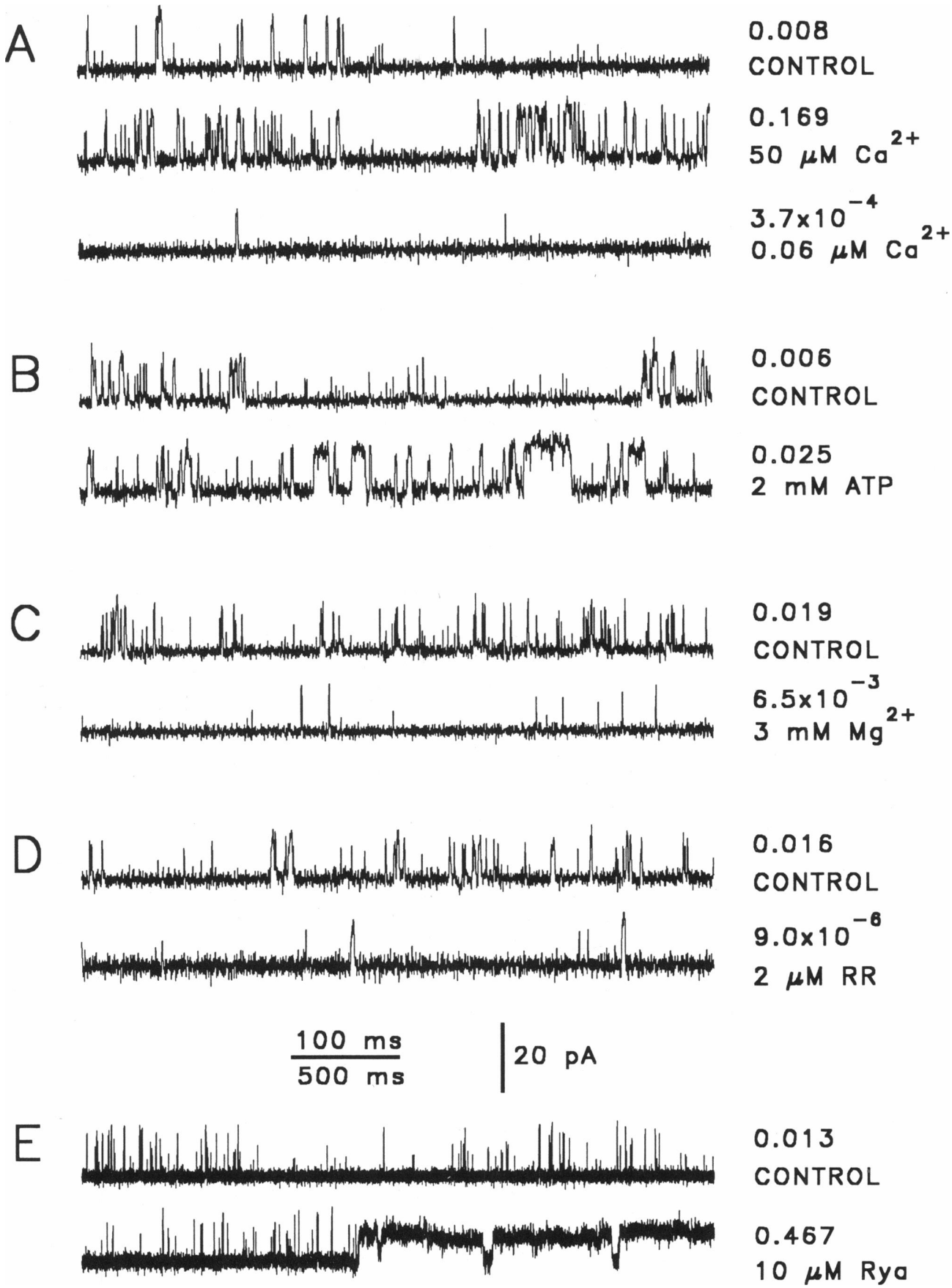
A
0.008
CONTROL
0.169
50 μM Ca2+
3.7x10-4
0.06 μM Ca2+
B
0.006
CONTROL
0.025
2 mM ATP
C
0.019
CONTROL
6.5x10-3
3 mM Mg2+
D
0.016
CONTROL
9.0x10-6
2 μM RR
100 ms
500 ms
20 pA
E
0.013
CONTROL
0.467
10 μM Rya

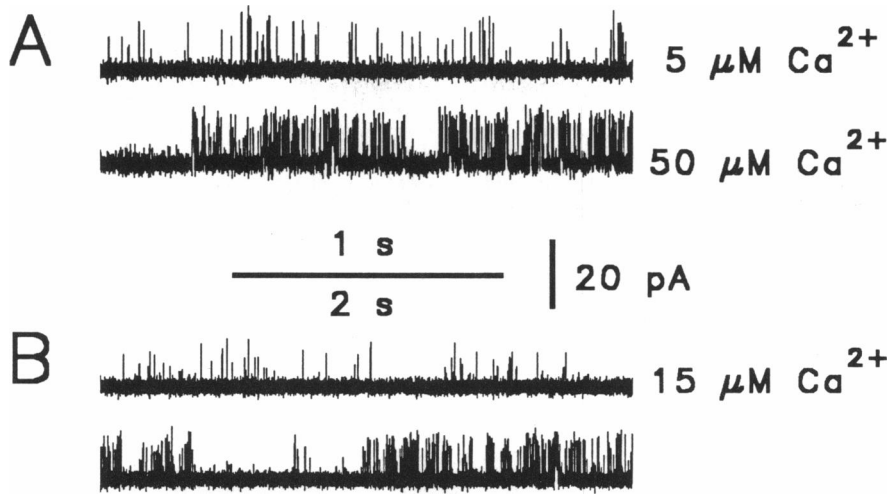

FIGURE 2 Cardiac sarcoplasmic reticulum Ca^{2+} release channels can gate both in an apparently random fashion as well as exhibit bursting behavior. (*A*) A short example of the change in channel gating mode caused by changing *cis*-Ca^{2+} concentration. (*Upper*) Random gating with 5 μM free Ca^{2+} present on the *cis* side of the bilayer. (*Lower*) Bursting behavior after adding calcium to the *cis* side of the bilayer to a final concentration of 50 μM. Channel activity was recorded with *cis* 250 mM $CsCH_3SO_3$ and *trans* 50 mM $CsCH_3SO_3$ at pH 7.4 and 0 mV. (*B*) Two samples lasting 4 s each from a bilayer containing only one Ca^{2+} release channel demonstrate random activity (*upper*) interspersed with apparent bursting behavior (*lower*). Conditions as in *A*; *cis* [Ca^{2+}] = 15 μM. Note different time calibration.

frozen in liquid nitrogen or at −70°C. Most experiments were carried out with the heavier (8,000 *g*) microsomal fraction despite its greater mitochondrial contamination and lower ryanodine binding (0.65 vs. 1.1 pmol/mg for the 40,000 *g* fraction) since it appeared to yield more successful incorporations of the calcium release channel.

Planar lipid bilayers consisting of 5:3:2 phosphatidyl ethanolamine/phosphatidyl serine/phosphatidyl choline (Avanti Polar Lipids, Birmingham, AL) were formed across a 150 μm diameter aperture in a Teflon chamber using a 50 mg/ml mixture of the phospholipids in decane (Gold label, Aldrich Chemical Co., Milwaukee, WI). Both sides of the aperture were initially bathed with 50 mM $CsCH_3SO_3$, 5 mM CsMOPS (3-(*N*-morpholino)-propane sulfonic acid), pH 7.4, 5 μM Ca^{2+} (this concentration was high enough for membrane stabilization). After bilayer formation, 200–500 μg of sarcoplasmic reticulum microsomal protein was added to the *cis* side (1.5 ml solution volume) and gently stirred for 5 min. Then $CsCH_3SO_3$ from a concentrated stock solution was added to the *cis* side of the bilayer to achieve a final concentration of 250 mM and induce vesicle incorporation into the bilayer. By convention, the *cis* side of the bilayer is defined as the side to which microsomal vesicles and higher salt concentrations are added. We have grounded the bath on the *cis* side and applied potential steps of varying duration to the *trans* side, opposite to the convention used in most laboratories, as in our hands it increased the stability of the bilayer to solution additions to the *cis* side. To maintain conventions, the potentials given throughout this article are those experienced at the *cis* (cytoplasmic) side relative to the *trans* (lumenal) side.

The calcium concentration in experimental solutions (contaminating level = 2–3 μM) was adjusted using 2 mM calcium methanesulfonate or 2 mM Cs_2ethyleneglycol-bis(β-aminoethyl ether)-*N*,*N*′-tetraacetic acid (EGTA). Calculations of the necessary amount of EGTA were performed according to Fabiato and Fabiato (41). In all experimental solutions the calcium concentration that was actually achieved was measured by a Ca-ion selective electrode (Orion Research Inc., Cambridge, MA) calibrated with the use of commercial standard solutions (WPI Inc., Sarasota, FL).

Bilayer measurements and analysis

The bilayer amplifier was based on the design described in Hamilton et al. (42). Bilayer recordings were stored on VCR tape using a modified Sony PCM 501ES digital audio processor (Unitrade, Inc., Philadelphia, PA); replayed data were filtered with a low pass 8-pole Bessel filter (902LPF, Frequency Devices, Haverhill, MA) at 2 kHz and digitized at 5 kHz using a TL-125 interface with pCLAMP software (programs CLAMPEX and FETCHEX, Axon Inst., Foster City, CA). Analysis and simulations were carried out on an IBM AT clone using pCLAMP (FETCHAN and pSTAT), IPROC and CSIM software (Axon Inst.) and MathCAD 2.50 (Mathsoft, Cambridge, MA). For determination of conductance, I–V curves were measured with 1-s long pulses to −50 · · · +50 mV (in 10-mV steps). Amplitudes of all fully resolved open events were measured using CLAMPEX or FETCHAN, and their mean was used. For testing possible amplitude differences

FIGURE 1 Cs^+-conducting canine cardiac microsomal membrane channels incorporated into planar lipid bilayers display all the properties expected of sarcoplasmic reticulum Ca^{2+} release channels. All recordings were obtained at pH 7.4 with 250 mM $CsCH_3SO_3$ on the *cis* side of the bilayer and 50 mM $CsCH_3SO_3$ on the *trans* side of the bilayer at a holding potential of 0 mV. All openings are upward. Numbers to the right of the traces indicate the open probabilities calculated for longer stretches of data under each condition. (*A*) Reversible activation of the channel by increase in *cis* (cytoplasmic) free [Ca^{2+}] from 3 to 50 μM, followed by a decrease of channel activity after addition of EGTA to reduce free [Ca^{2+}] to 0.06 μM, as indicated. (*B*) Activation of channel activity by ATP. Activity of a single channel in the presence of 15 μM *cis* Ca^{2+} alone (above) and after subsequent addition of 2 mM Na_2ATP. (*C*) Inhibition of channel activity by millimolar *cis* Mg^{2+}. Activity of a single channel in the presence of 15 μM *cis* Ca^{2+} alone (above) and after addition of 3 mM $MgSO_4$ (below). (*D*) Inhibition of channel activity by micromolar *cis* ruthenium red. Activity of a single channel in the presence of 10 μM Ca^{2+} alone (above) and after addition of 2 μM ruthenium red (below). (*E*) Effect of ryanodine. Activity of a single channel in the presence of 10 μM *cis* Ca^{2+} alone (above) and shortly after addition of 10 μM ryanodine (below). Note different time calibration.

between channels under control conditions and after adding procaine, event amplitudes were measured at −50 and 0 mV. Data segments lasting 60–200 s were used for analysis of open probability and single-channel kinetics. The number of openings was 5,000–13,000 under control conditions and proportionally less after adding procaine. Open and closed times were measured by IPROC after digital filtering at 1,500 Hz with the discriminator level set at 50% of the current amplitude. As events shorter than twice the dead time, which equals 120 μs for a Gaussian filter set at 1,500 Hz, are underestimated with 50% detection (43), events shorter than 400 μs (two sample intervals) were not included in the analysis. Open probability P_O was measured as the sum of all open times divided by the total time. The events lists generated by IPROC were analyzed using the program pSTAT, which created and fitted noncumulative histograms of dwell times. The number of exponential components in the distributions of event durations was determined by comparing χ^2 of fits with sequentially increasing number of components. The larger number of components was judged to improve the fit significantly if χ^2 was decreased $\geq$10 times by increasing the number of components (the usual values were 20–1,000 times). The areas and time constants of individual exponential components resulting from this analyses are corrected for missed events.

For illustration purposes, records longer than 5 s per trace were plotted after digital refiltering at 500 Hz and resampling at 1 kHz, which had no adverse effects on record appearance.

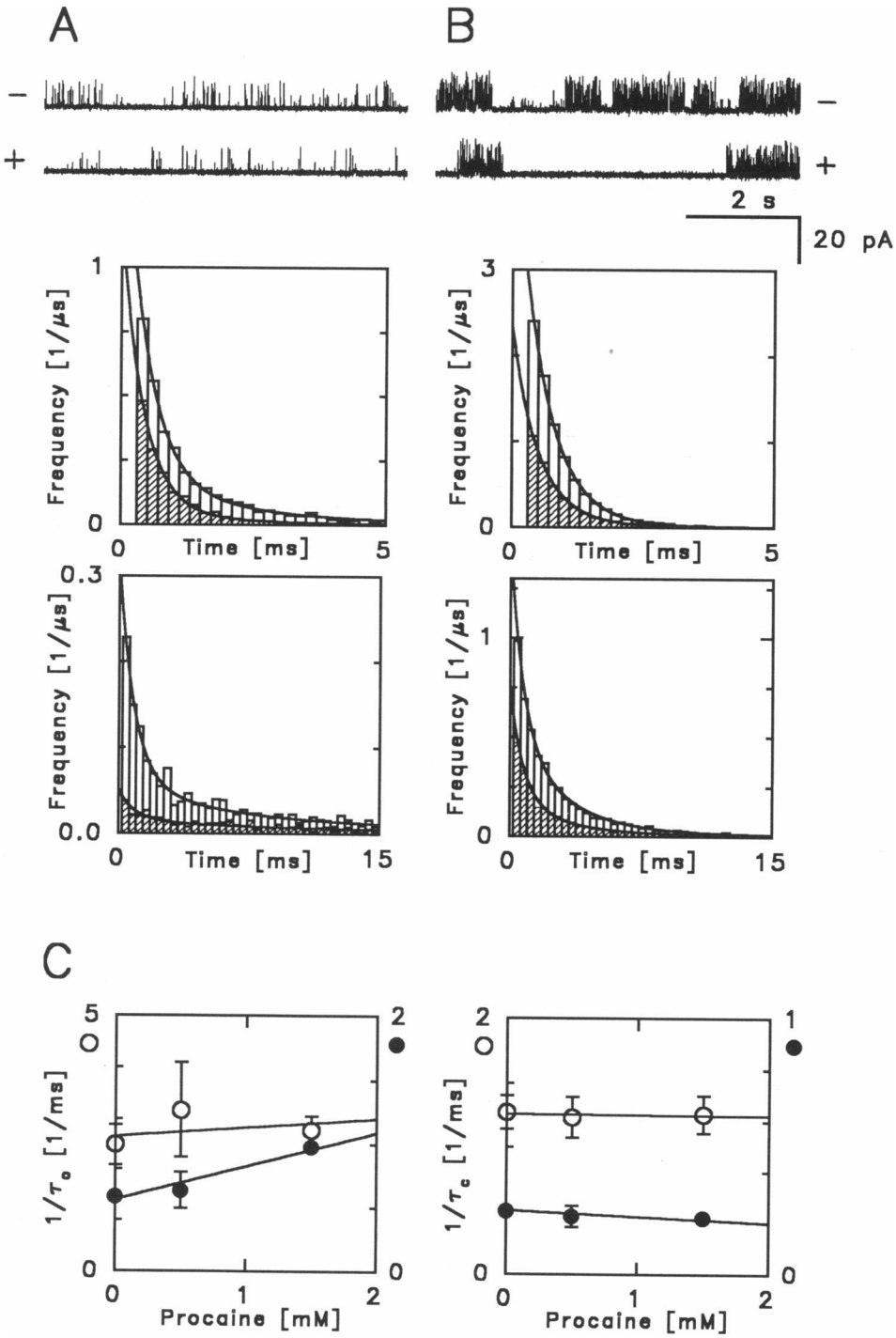

Modeling channel open probabilities and kinetics

The equilibrium open probabilities P_O for individual models were calculated as analytical functions of calcium and procaine concentration using the law of mass action. The equilibrium constants were chosen so that maximal open probability at 100 μM activating Ca^{2+} was P_O^{max} = 0.15 − 0.25 (1, 44). Activation by calcium was considered to be a 1:1 reaction of Ca^{2+} with the resting state, so that

$$P_O = P_O^{max} \times [Ca^{2+}]/(K_{Ca} + [Ca^{2+}]), \quad (1)$$

and its rate constant was adjusted to give an effective binding constant K_{Ca} = 3 μM. Inhibition by procaine was considered to be a 1:1 reaction with one or more of the states. Results were expressed as P_{rel}, the open probability of the channel at a given calcium concentration in the presence of procaine relative to that in the absence of procaine under otherwise the same conditions. Depending on the model used, the inhibition was independent of Ca^{2+} at certain limiting conditions (either $[Ca^{2+}] \rightarrow \infty$ or $[Ca^{2+}] \rightarrow 0$). Under these limiting conditions, the procaine concentration dependence of the inhibitory reaction can be expressed as

$$P_{rel} = K_{Proc}/(K_{Proc} + [Proc]). \quad (2)$$

The rate constant(s) for the reaction(s) with procaine were chosen so that the effective binding constant K_{Proc} was equal to the value observed experimentally. The calculations were performed using the program MathCAD.

The equilibrium probabilities of individual states and proposed open and closed time constants of the channel under control conditions (without procaine) were chosen in approximate accordance with published data (1) and with our experimental data. They were used to build a set of equations, describing the equilibria between channel states as ratios of transition rates and the time constants as sums of transitions rates (45) for the models examined. The set of equations was solved using the program MathCAD. All combinations of assigning channel states to time constants were tested. The matrices of transition rates corresponding to individual gating models were then used in two ways. First, the effects of procaine binding to individual channel states on the observed time constants at different calcium concentrations were theoretically calculated by means of eigenvalue analysis (45, 46) using MathCAD. Second, channel kinetics were simulated with the program CSIM. Data files lasting 2–5 min with parameters close to the experimental ones (conductance of 400 pS, reversal potential of −40 mV, 1.5 pA r.m.s. noise, sampling frequency 5 kHz, filtering at 1,500 Hz) were generated. The simulated files were analyzed with IPROC and pSTAT using the same parameter settings as for the experimental data.

TABLE 1 Kinetic parameters of calcium release channels

	Parameters of time distributions			
	Open time distribution		Closed time distribution	
Procaine	τ	Area	τ	Area
mM	*ms*	%	*ms*	%
0 (n = 5)	0.44 ± 0.05	67 ± 7	0.82 ± 0.09	35 ± 4
	1.56 ± 0.14	33 ± 7	4.02 ± 0.47	39 ± 6
			22 ± 3	26 ± 6
0.5 (n = 4)	0.42 ± 0.05	74 ± 12	0.84 ± 0.11	17 ± 7
	1.47 ± 0.20	26 ± 12	4.90 ± 0.68	27 ± 6
			78 ± 35	56 ± 13
1.5 (n = 5)	0.44 ± 0.04	74 ± 8	0.69 ± 0.11	22 ± 6
	1.09 ± 0.10	26 ± 8	4.63 ± 0.52	32 ± 10
			54 ± 9	54 ± 9

Values are means ± SEM. Data pooled from experiments at 5, 15, and 100 μM Ca^{2+}.

RESULTS AND DISCUSSION

Canine cardiac sarcoplasmic reticulum Ca^{2+} release channels readily incorporate into planar lipid bilayers even from relatively crude unpurified cardiac microsomal preparations. Under the recording conditions utilized, other kinds of channels do not appear to contribute to the records obtained, probably because sarcoplasmic reticulum K^+ and Cl^- channels as well as sarcolemmal Na^+, K^+, and Cl^- channels are poorly permeable to Cs^+ and $CH_3SO_3^-$ (47). Contributions due to Cs^+ flux through either T- or L-type sarcolemmal Ca^{2+} channels are likely to be minor due to (*a*) inactivation of these channels at a holding potential of 0 mV (48), (*b*) the much smaller single channel conductance of these

FIGURE 3 Effect of procaine on single cardiac sarcoplasmic reticulum Ca^{2+} release channels. Channel activity was recorded with *cis* 250 mM $CsCH_3SO_3$ and *trans* 50 mM $CsCH_3SO_3$ at pH 7.4 and 0 mV. Refiltered at 500 Hz; resampled at 1 kHz. (*A*) Channel exhibiting random openings with 5 μM Ca^{2+} present on the *cis* (cytoplasmic) side of the bilayer. The first row demonstrates control channel activity before procaine addition; the second row demonstrates activity in the presence of 0.5 mM procaine added to the *cis* side of the bilayer. (*Third row*) Histograms of channel open times in control (*open bins*) and in the presence of 0.5 mM procaine (*hatched bins*). The theoretical distributions of opening frequency are as follows: control, $f[\mu s^{-1}] = 1.99 \exp(-t/0.45) + 0.18 \exp(-t/2.30)$; procaine, $f[\mu s^{-1}] = 1.44 \exp(-t/0.45) + 0.044 \exp(-t/2.30)$. (*Fourth row*) Histograms of channel closed times in control (*open bins*) and in the presence of 0.5 mM procaine (*hatched bins*). The theoretical distributions of closing frequency are as follows: control, $f[\mu s^{-1}] = 0.29 \exp(-t/0.85) + 0.053 \exp(-t/5.8) + 0.013 \exp(-t/34)$; procaine, $f[\mu s^{-1}] = 0.038 \exp(-t/0.85) + 0.013 \exp(-t/5.8) + 0.005 \exp(-t/75)$. (*B*) Another channel exhibiting bursting channel activity with 100 μM Ca^{2+} present on the *cis* side of the bilayer. The first row demonstrates control channel activity before procaine addition; the second row activity in the presence of 0.5 mM procaine. (*Third row*) Histograms of channel open times in control (*open bins*) and in the presence of 0.5 mM procaine (*hatched bins*). The theoretical distributions of opening frequency are as follows: control, $f[\mu s^{-1}] = 5.99 \exp(-t/0.52) + 0.081 \exp(-t/1.90)$; procaine, $f[\mu s^{-1}] = 2.75 \exp(-t/0.52) + 0.076 \exp(-t/1.90)$. (*Fourth row*) Histograms of channel closed times in control (*open bins*) and in the presence of 0.5 mM procaine (*hatched bins*). The theoretical distributions of closing frequency are as follows: control, $f[\mu s^{-1}] = 1.03 \exp(-t/0.82) + 0.53 \exp(-t/3.45) + 0.018 \exp(-t/13.7)$; procaine, $f[\mu s^{-1}] = 0.62 \exp(-t/0.82) + 0.16 \exp(-t/3.45) + 0.001 \exp(-t/176)$. In both examples procaine reduced the number of openings. (*C*) Procaine dependence of channel open times and the two shorter closed times. Individual points are means ± SEM of four to five experiments. Continuous lines are linear regressions. Note that two separate ordinates apply to each panel, the left for the open circles and the right for the filled circles, with maximal values in 1/ms indicated above the circles. (*Left*) *Open circles,* short open time, R = 0.19; *closed circles,* long open time, R = 0.75. (*Right*) *Open circles,* short closed time, R = 0.21; *closed circles,* medium closed time, R = 0.26.

channels even when conducting monovalent cations (30 pS, skeletal t-tubule L-type channels [49]; 45–100 pS, cardiac L-type Ca channels [50, 51]; 26 pS, cardiac T-type Ca channels [52]), and (*c*) the presence of sufficient Ca^{2+} (≥ 3 μM) on the *cis* side of the bilayer to reduce passage of monovalents through such channels (53–55). We did frequently experience large sudden shifts in the baseline of our recordings that might have been due to incorporation of relatively nonselective mitochondrial VDAC channels (56); when any additional

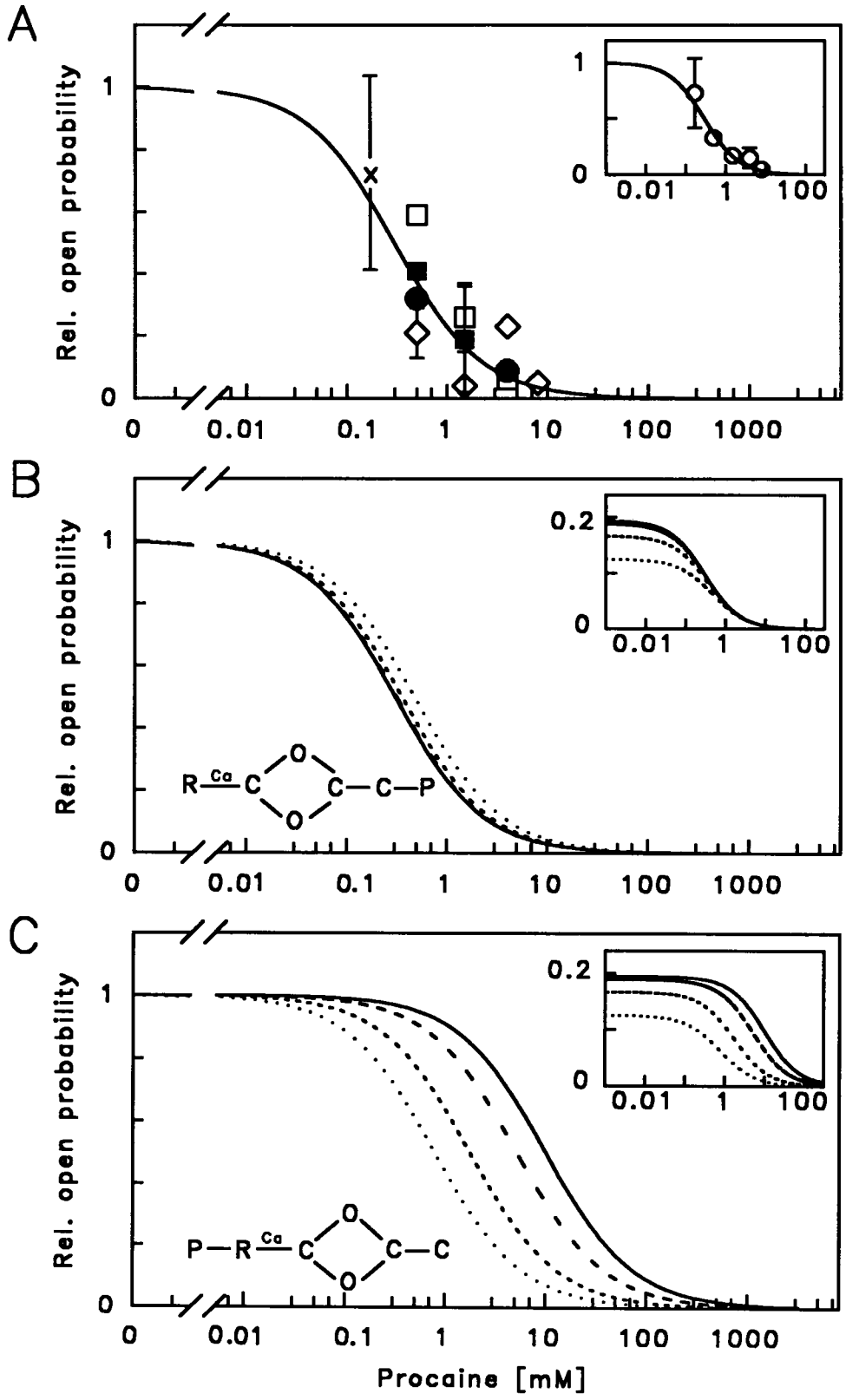

non-Ca^{2+} release channel gating was observed, experiments were terminated.

Typical recordings of cardiac Ca^{2+} release channels are shown in Fig. 1. Short openings in these and other records appear clipped due to filtering. Under our recording conditions the channels exhibit a γ_{Cs} of 441 ± 12 pS (n = 22), similar to that reported for skeletal Ca^{2+} release channels under similar ionic conditions (rabbit, 500 ± 12 pS [2]; normal pig, 438 ± 34 pS; malignant hyperthermic pig, 383 ± 24 pS [47]) and practically equal to the value reported for sheep cardiac Ca^{2+}-release channels in symmetrical 210 mM CsCl (440 ± 8 pS [57]). The channels recorded under these conditions (Fig. 1) are clearly Ca^{2+} release channels, as evidenced by their pharmacological sensitivity: *cis* activation by micromolar [Ca^{2+}] and by ATP, block by millimolar Mg^{2+} or micromolar ruthenium red, and induction of a long-lived substate by ryanodine (*A* to *E*, respectively).

We routinely observed two types of kinetic behavior, which we have termed "random" and "bursting," on the part of the Ca^{2+} release channel. We have observed a tendency toward what we refer to as "random" gating (Fig. 2 *A*, *upper trace*) when the *cis* free [Ca^{2+}] is low and a greater likelihood of observing "bursting" behavior when the *cis* free [Ca^{2+}] is elevated (Fig. 2 *A*, *lower trace;* both records are from the same channel). Both forms of gating can be seen in a single channel bilayer at moderate *cis* [Ca^{2+}] (15 μM, Fig. 2 *B*, no multiple openings observed during 4 min of continuous recording). More commonly, we have observed each type of behavior separately at low or high [Ca^{2+}] in single channel bilayers or both forms of gating together at intermediate [Ca^{2+}] in multichannel bilayers (not shown).

Procaine effect on the Ca^{2+} release channel

Procaine affected both forms of gating of the channel but not its conductance; no high frequency flicker block was observed at 0 mV. As seen in Fig. 3 *A* with a "randomly" gating channel, procaine reduces the number of openings per unit time without a marked change in the appearance of individual openings at this time resolution. The decrease in open probability from P_O = 0.03 in the control (*first panel*) to P_O = 0.01 in the presence of 0.5 mM procaine (*second panel*) clearly appears to be due primarily to a decreased frequency of channel openings. A similar effect of procaine is observed on channels that exhibit bursting behavior (Fig. 3 *B*, from P_O = 0.18 to P_O = 0.06). The number of openings is reduced and the duration and frequency of long closures increases.

To examine more quantitatively the characteristics of the blocking events produced by procaine, we have performed standard kinetic analysis of open and closed times on both forms of Ca^{2+} release channel gating be-

FIGURE 4 Dose-response relationship for procaine reduction of cardiac sarcoplasmic reticulum Ca^{2+} release channel open probability. The open probability is normalized to that in the absence of procaine. (*A*) Summary of experimental dose-response behavior in channels activated by different *cis* free Ca^{2+} concentrations, 5 μM (*diamonds*), 15 μM (*squares*), and 100 μM (*circles*), and exhibiting random (*open symbols*) or bursting (*closed symbols*) behavior. Where brackets are given, these represent SEM of three or more experiments. The × symbol at 0.17 mM procaine represents pooled data from four experiments at a *cis*-[Ca^{2+}] of 5 and 15 μM. The continuous curve represents a fit of pooled data to the equation: $P_{rel} = 1/(1 + ([Proc]/K_{Proc}))$, with K_{Proc} = 0.30 ± 0.10. (*Inset*) Pooled dose-response curve obtained by averaging the data at all conditions. Theoretical curve is identical with the above one. (*B*) Simulated effects of procaine on relative open probability as a function of free [Ca^{2+}] for a model in which procaine binds only to one of the Ca^{2+}-bound closed states of the channel (C). Simulations are normalized to the open probability of the channel under the same conditions but in the absence of procaine (as in *A*). Inset at lower left shows schematically the gating scheme (R = resting, Ca-free state; C = closed, Ca-bound state; O = open, Ca-bound state; P = closed, procaine-bound state); inset at upper right shows the same data as absolute values of open probability. Simulated Ca^{2+} concentrations are as follows: *dot*, 5 μM; *small dash*, 15 μM; *long dash*, 50 μM; *solid line*, 100 μM. The apparent binding constants for activation by Ca and inhibition by procaine are, respectively, K_{Ca} = 3 μM and K_{Proc} = 0.3 mM. The small shift in sensitivity is due to increasing availability of state C3 to procaine at higher [Ca^{2+}]. The following relationship holds for the dependence of open probability on the concentrations of Ca^{2+} and procaine:

$$P_O = P_O^{max} \times \frac{[Ca]}{[Ca] + K_{Ca}\dfrac{K_{Proc}}{K_{Proc} + [Proc]}} \times \frac{K_{Proc}}{K_{Proc} + [Proc]}. \quad (5)$$

(*C*) Simulated effects of procaine on relative open probability as a function of free [Ca^{2+}] for a model in which procaine binds to the resting state of the channel (R), the same state to which Ca^{2+} binds. Simulations are normalized as in *A* and *B*. Inset at lower left shows schematically the gating scheme; inset at upper right shows the same data as absolute values of open probability. Simulated Ca^{2+} concentrations are designated as in *B*. The apparent binding constants for activation by Ca and inhibition by procaine are, respectively, K_{Ca} = 3 μM and K_{Proc} = 0.3 mM. In this case the relationship between open probability of the channel and the concentrations of Ca^{2+} and procaine are:

$$P_O = P_O^{max} \times \frac{[Ca]}{[Ca] + K_{Ca} \times \dfrac{K_{Proc} + [Proc]}{K_{Proc}}}. \quad (6)$$

Note that the former model leads to noncompetitive behavior between procaine and Ca^{2+}, whereas the latter model predicts strictly competitive behavior in which high [Ca^{2+}] reduces the sensitivity toward procaine. Note that there is no relationship to be made between the insets at the upper right of the three panels.

fore and after application of procaine. As seen in Fig. 3 *A*, two open times (*third panel*, open bins) and three closed times (*fourth panel*, open bins) are required to fit the data of a randomly gating channel in the absence of procaine. In the presence of 0.5 mM procaine, there was no measurable change in channel mean open times in this experiment, although the areas of both exponential components were reduced (Fig. 3 *A*, *third panel, hatched bins*), indicating that fewer openings occurred. Similarly, the short channel closed times remained unchanged in the presence of procaine (Fig. 3 *A*, *fourth panel, hatched bins*), whereas the very slow closed time constant was increased (Fig. 3 *A*). The increase in the proportion of long closed times and resulting reduction in the number of openings per unit time contributes significantly to the reduction in open probability exerted by procaine on randomly gating Ca^{2+} release channels.

A similar analysis was performed on a bursting Ca^{2+} release channel in Fig. 3 *B* before and after procaine application. As with randomly gating channels, the effect of procaine on open time distribution is primarily to reduce the number of openings without affecting their duration (*third panel*). Similarly, the effects on the measured closed time distribution were to decrease the number of short and medium closures (*fourth panel*). The duration of long closures seems to be significantly prolonged (Fig. 3 *B*). Since neither the two open times nor the two shorter closed times are appreciably changed, the effects of procaine on bursting as well as random channel gating appear to be nearly entirely mediated by a decrease in the number of short openings and closures per unit time at the expense of an increase in the number and duration of very long closures.

Possible small effects on the two open and the two shorter closed times were analyzed from five channels with procaine concentrations up to 1.5 mM (Table 1). Both open and closed times are shorter than reported by Ashley and Williams (1), possibly because of a higher bandwidth (1,500 Hz) of our recordings and/or use of Cs^+ as a conducting ion. As plotted in inverse form in Fig. 3 *C*, the two shorter closed times tend to increase (*left*) and the two open times tend to decrease (*right*) as [procaine] is increased. Both effects would decrease the channel open probability. For both closed times τ_{C1} and τ_{C2} and the short open time τ_{O1} the effect was not significant (the correlation coefficient R for the equation $1/\tau_i = A + [\text{Proc}]/B$ was $R < 0.3$). The longer open time constant does seem to vary as a function of the procaine concentration, but the changes are relatively small ($1/\tau_{O2} = 0.55 + [\text{Proc}]/K^{\tau}_{\text{Proc}}$; $K^{\tau}_{\text{Proc}} = 4.3$ mM, $R = 0.75$). Procaine is almost 15 times less effective in reducing the longer open time than in reducing the open probability. Shortening of channel openings can contribute at most 19% to the total effect in 1.5 mM procaine and only 12% to the total effect in 0.5 mM procaine.

The long closed times are significantly prolonged in the presence of procaine. However, the precision of the long closed time is very low (Table 1), and, without a commercially available program for maximum likelihood analysis, we were not able to improve it by any changes in the way of binning the histograms. Since none of the other more measurable time constants was appreciably affected, the decrease in P_O induced by procaine appeared due to long closures, which accounted for most of the time the channel was closed (Table 1).

In Fig. 4 *A*, P_O data as a function of [procaine] from a total of 13 channels were divided into four categories according to their *cis* Ca^{2+} concentration and random or bursting behavior (different symbols). The theoretical curve is a fit to pooled data ($K_{\text{Proc}} = 0.30 \pm 0.10$, mean $\pm$ SD of the fit). Although the data do indicate a substantial scatter in the results, there does not appear to be any overall trend to the data that would suggest that the sensitivity of the channel to procaine is markedly affected by variation in *cis* [Ca^{2+}] from 3 to 100 μM or whether the channel exhibits a random or bursting form of gating. Were the sensitivity to procaine affected by either of these factors, we would have expected points involving those conditions to fall either all substantially to the right or all substantially to the left of the curve fitted to all the data as a simple 1:1 inhibitory effect. There were no statistically significant differences between the relative open probabilities of random and bursting groups (six channels in the presence of 0.5 and 1.5 mM procaine) or between groups with *cis* Ca^{2+} concentration of 3 and 15 μM (five channels in the presence of 0.5 mM procaine). When all four categories are pooled together, the scatter of the data is reduced (see *inset*, Fig. 4 *A*).

Modeling the Ca^{2+} release channel–procaine interaction

Previous analyses of the cardiac sarcoplasmic reticulum Ca^{2+} release channel kinetics have suggested a minimal gating model (1) that is summarized in Eq. 3:

$$Ca^{2+} + R \rightleftharpoons \begin{matrix} & O1 & \\ C1 & & C2 \\ & O2 & \end{matrix}. \qquad (3)$$

Ashley and Williams (1) identified three closed time components with time constants that were dependent on Ca^{2+} concentration, but their relative areas were found to be only weakly dependent on Ca^{2+} in the range 0.01–100 μM Ca^{2+} (short, 45–65%; intermediate, 29–42%; long, 6–14%). They found that the states C1 and C2 have lifetimes on the order of 1–10 ms and can be related to the two shorter closed time components.

From the gating scheme shown in Eq. 3, it can be inferred that at low Ca^{2+}, the lifetime of the resting state R is long, and the channel spends most of the time in it. As Ca^{2+} is increased, both the population and the lifetime of state R should decrease to very low values. To account for long closures at higher Ca^{2+} concentrations (when the lifetime of state R decreases dramatically), an additional closed state that contributes to the long closed

time component has to be postulated. For this reason we included a third closed Ca^{2+}-bound state C3 into the above scheme:

$$Ca^{2+} + R \rightleftharpoons \begin{matrix} \nearrow O1 \searrow \\ C1 \qquad C2 \rightleftharpoons C3. \\ \searrow O2 \nearrow \end{matrix} \qquad (4)$$

The interaction of procaine with the channels manifests itself mainly as prolongation of long closures at both low and high *cis* $[Ca^{2+}]$ and as a large increase in their relative number at low *cis* $[Ca^{2+}]$. These closures probably do not originate by binding of procaine to the open Ca^{2+} release channel (sites O1 and O2), because the effect of procaine on channel open times contributes <20% to the total effect (Fig. 3 *C, left*), and the open time is almost 15 times less dependent on procaine concentration than is the open probability.

Thus, interaction with closed states predominates in the action of procaine on Ca^{2+} release channels. The short-lived closed states C1 and C2 appear little affected (Fig. 3 *C*). The remaining closed states R and C3 are both likely candidates at first consideration. At low $[Ca^{2+}]$ (Fig. 3 *A*), both of these states are long lived, and their interaction with procaine would result in affecting the duration of long closures and an increase in their proportion. At high $[Ca^{2+}]$ (Fig. 3 *B*), the small number and long duration of the long closures could be attributed to either long-lasting procaine binding to state R (which is accessible only rarely) or to procaine binding to the long-lived state C3.

Using the scheme of Eq. 4, we modeled the effects of permitting procaine to interact at these two sites (Fig. 4, *B* and *C*). The first model (Fig. 4 *B*) assumes interaction of procaine (P) with state C3; in the second model (Fig. 4 *C*) procaine interacts with state R. The open probability relative to P_O in the absence of procaine is plotted as a function of procaine concentration in the same fashion as for the experimental data in Fig. 4 *A* for different levels of activating Ca^{2+} (the different curves). The model was calculated as a chemical equilibrium according to Eq. 4, with the equilibrium constants chosen so that $P_O^{max} = P(O1)^{max} + P(O2)^{max} = 0.2$ at maximal activating Ca^{2+}. The values of K_{Ca} and K_{Proc}, the effective binding constants for Ca^{2+} and procaine, were set to 3 μM and 0.3 mM, respectively.

In Fig. 4 *B*, selective interaction of procaine with closed state C3 generates curves of procaine inhibition of the channel that are nearly insensitive to $[Ca^{2+}]$ at activating Ca^{2+} concentrations ($[Ca^{2+}] \geq 5$ μM), as experimentally observed (Fig. 4 *A*). If procaine interacted selectively with state R (Fig. 4 *C*), then increasing $[Ca^{2+}]$ would shift the sensitivity of the channel to procaine in a competitive manner, contrary to the experimentally observed Ca^{2+} insensitivity.

The lack of interaction between procaine and Ca^{2+} also suggests that nonspecific screening of membrane phospholipid surface charge (e.g., McLaughlin and Whitaker [58]) is unlikely to play a significant role in the inhibitory effects of procaine on the Ca^{2+} release channel. However, a nonspecific interaction between procaine, the hydrophobic core of membrane phospholipids, and the channel protein, similar to the interaction of some class III antiarrhythmic drugs and dihydropyridine receptors (59), cannot be ruled out unequivocally.

We also wished to determine whether the scheme of Eq. 4 with procaine binding to C3 could reproduce our basic kinetic findings, including different forms of gating equally sensitive to procaine. Using the time constants and area ratios determined in the experiments (Table 1, Fig. 3) as an approximate starting point, we simulated channel activity (using the program CSIM) according to the basic scheme outlined above. We did not attempt to create a model that exactly reproduced the observable open and closed times but rather one that followed the trends observed experimentally. The "pattern" characteristics were determined visually from the traces plotted in the same way as experimental data; open probabilities and kinetic characteristics were determined as in the case of experimental data. The basic criteria that were met by the model included the following.

(*a*) At low $[Ca^{2+}]$, appearance of random openings with $P_O \leq 0.05$ and only rare and very short bursts (Fig. 5 *A, upper trace*).

(*b*) At high $[Ca^{2+}]$, appearance of long clusters of bursts separated by long gaps, with $P_O \leq 0.2$ (Fig. 5 *A, second trace*).

(*c*) At intermediate $[Ca^{2+}]$, appearance of both random openings and bursts, with strongly varying proportion of bursts from one 1-min segment to another (Fig. 5 *B*).

The rate constants used for the simulations are given in Table 2. Several basic prerequisites for generating gating that approximated the one observed experimentally (cf. Fig. 2 experiment with Fig. 5, *A* and *B* model) had to be met. The rate of Ca^{2+} dissociation k_{C1R} had to be sufficiently high (100 s^{-1} or more) to create the random pattern at low calcium concentrations ($Ca^{2+} = 5$ μM). The transitions between states O1 and C2 and between states O2 and C1 had to be slow (on the order of s^{-1}). The fastest transitions, experimentally observable in the histograms as τ_{O1} and τ_{c1}, had to connect states O2 and C2. The C3 state had to be connected to C2 to produce the correct gating pattern. If the three closed, Ca^{2+}-bound states C1, C2, and C3 were arranged in any other way than in Eq. 4, then the resulting channel activity either did not show both (random and bursting) types of gating or the calcium dependence of this behavior was altered. The transition between states C2 and C3 had to be slow, with the equilibrium shifted to the side of C3.

At low and medium calcium concentrations, bursts consist of sojourns in states O2 and C2, and during a stretch of random openings the channel flips between states R, C1, and O1. Bursts are sparse and relatively short at low Ca^{2+}. Long closures into the state C3 are

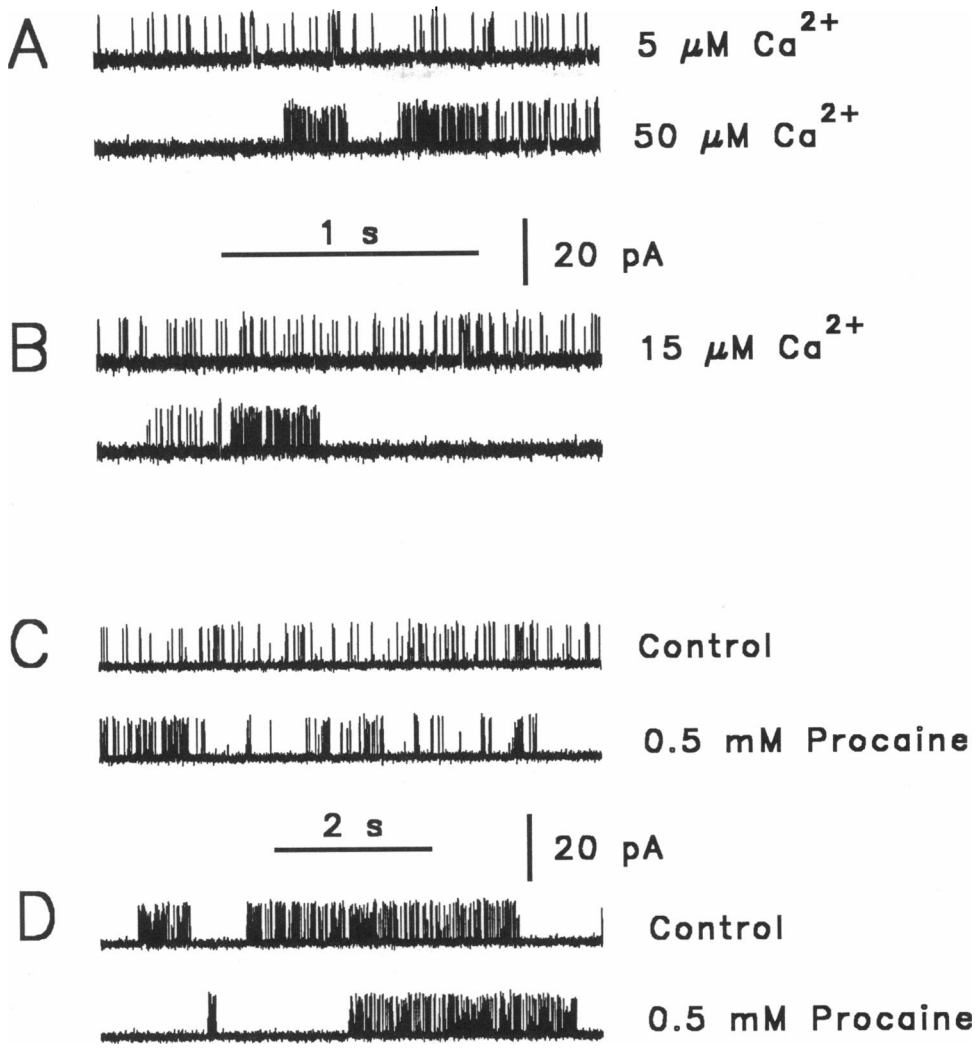

FIGURE 5 Simulated single channel behavior according to the model presented in the text. (*A*) Channel activity at different activating Ca^{2+} concentrations. (*Upper*) 5 μM Ca^{2+}; (*lower*) 50 μM Ca^{2+}. Bursting behavior is more apparent at higher Ca^{2+} concentrations. Filtered at 1500 Hz. (*B*) Two samples lasting 3 s each from a simulation of the activity of one Ca^{2+} release channel at 15 μM Ca^{2+} demonstrate gearshifting between random activity (*upper*) interspersed with apparently bursting behavior (*lower*). Filtered at 1,500 Hz. (*C*) Channel activity with 5 μM *cis* [Ca^{2+}] in the absence of procaine (*upper*) and in the presence of 0.5 mM procaine (*lower*). The rate constants for the reaction C3 ⇄ *P* were k_{C3P} = 30.1 $M^{-1} \cdot s^{-1}$ and k_{PC3} = 5 s^{-1}. Filtered at 500 Hz; resampled at 1 kHz. (*D*) Channel activity with 100 μM *cis* [Ca^{2+}] in the absence of procaine (*upper*) and in the presence of 0.5 mM procaine (*lower*). The rate constants for the reaction C3 ⇄ *P* were k_{C3P} = 30.1 $M^{-1} \cdot s^{-1}$ and k_{PC3} = 5 s^{-1}. Filtered at 500 Hz; resampled at 1 kHz.

also relatively rare. At high Ca^{2+} the occupancy of state R is very low, and all sojourns in states O1, C1, O2, or C2 appear as bursts, which are separated by longer closures after entering state C3.

Finally, simulations of the effects of procaine binding to the long-lived closed state C3 when the channels were respectively gating randomly or in bursting fashion are shown in Fig. 5, *C* and *D*, for comparison with the experimental results shown in Fig. 3, *A* and *B*. The open probabilities were in complete accord with the experimental data if sufficiently long (≥100 s) data files were simulated. The time constants and areas of individual open and closed time components after analysis with IPROC and FETCHAN were in qualitative agreement with the experimental data: only three closed time components could be resolved, the slowest one having the lowest precision.

We also compared the effect of procaine binding with either of the three closed states on the observable closed times. The rate constant of procaine unbinding was set to 5 s^{-1}, as in the simulations shown in Fig. 5, and the forward rate constant k_{CiP} (i = 1, 2, 3 for procaine binding to states C1, C2, or C3, respectively) was calculated to give an effective binding constant K_{Proc} of 0.3 mM ($k_{C1P} = 6.3 \times 10^4$ M^{-1} s^{-1}, $k_{C2P} = 1.5 \times 10^5$ M^{-1} s^{-1}, $k_{C3P} = 3.0 \times 10^4$ M^{-1} s^{-1}). The eigenvalue problem for the three respective submatrices of the matrix of transition rates (45) was solved using MathCAD as a tool. Procaine binding to C1, C2, or C3 induced the appearance of a very slow closed time component in the range

TABLE 2 **The rate constants used for the simulation of Ca^{2+}-release channel activity**

Rate constant*	Value
k_{RC1}‡ [$M^{-1} \cdot s^{-1}$]	17.6×10^6
k_{C1R} [s^{-1}]	200
k_{C1O1} [s^{-1}]	100
k_{C1O2} [s^{-1}]	1
k_{C2C3} [s^{-1}]	5
k_{C2O1} [s^{-1}]	1
k_{C2O2} [s^{-1}]	500
k_{C3C2} [s^{-1}]	1
k_{O1C1} [s^{-1}]	600
k_{O1C2} [s^{-1}]	2.52
k_{O2C1} [s^{-1}]	10
k_{O2C2} [s^{-1}]	2,100

* According to Eq. 4.

‡ The value of k_{RC1} was chosen to be of the same order of magnitude as the analogous rate constant in the Ca^{2+}-activated K channel model (67).

of seconds. Selective procaine interaction with states C1 or C2 always produced, in addition, a marked shortening of the corresponding shorter closed times (not shown) that was not observed experimentally, whereas binding of procaine to state C3 did not change the duration of the two shorter closed times.

On the basis of these results, we conclude that the most likely state to which procaine binds to the channel and produces the majority of its inhibitory effects on the channel activity is C3. The basic suitability of the model we have used appears to be confirmed by its remarkable ability to account for two novel forms of its gating behavior reported here: a Ca^{2+}-dependent transition or "gear-shifting" between two apparently different forms of channel gating and the influence of procaine on both forms of gating. That both these results could be obtained by only a one-state expansion of a kinetic scheme that was previously utilized to account for this channel's gating on a shorter time scale (1) further attests to its uniqueness. The ability of such a scheme to account for commonly observed nonstationary gearshift behavior is of great significance, in that phosphorylation or other slow modifications of this and other channels need not be invoked as explanations for such behavior.

We hasten to point out that notwithstanding our conclusion that the bulk of procaine's inhibitory effects on the Ca^{2+} release channel are exerted on state C3, our results do not preclude other forms of interaction between procaine and the channel. Clearly our own results indicating a small but significant effect on channel open times would suggest that other modes of interaction are possible. Our experiments have been carried out for the most part in the absence of adenosine triphosphate (ATP) or Mg^{2+}, ligands of great physiological significance. Thus, our scheme for the channel states is clearly a very simplified one relative to the states possible in situ.

Consequently, it may be premature to conclude that procaine's effects on the Ca^{2+} release channel are Ca^{2+}-insensitive under physiological conditions. Prior reports on this subject (28, 32, 60, 61) have arrived at mixed conclusions.

At neutral pH, procaine exists mainly in a charged form that appears responsible for its inhibitory effects on Ca^{2+} release (23, 31, 62). Since the affinity of the channel to procaine is low, we had anticipated that its effects would more likely be manifest as a high frequency flicker block similar to the action of local anesthetics on end plate channels (63) or Cd^{2+} on L-type Ca^{2+} channels (64). Our results suggest that procaine does not primarily interact with open channels and probably instead interacts preferentially with closed states of the channel. If the preferred closed state of the channel was an inactivated state as in the modulated receptor model for local anesthetic block of sodium channels (19), then this might also explain the decreased contracture durations observed by Heistracher and Hunt (24) on snake skeletal muscle fibers. The long-lived C3 state could be a likely candidate for such an inactivated state.

Thus, there clearly is no simple correlation between drug affinities and their mode of interaction with ion channels, even if such correlation may exist with certain blockers and certain channels (65). These results then clearly indicate that the on rate of interaction of procaine with the channel is considerably slower than diffusion limited. Had the on rate been diffusion limited, thermodynamic constraints also would have dictated that its dwell time on the channel would have been much shorter than observed. Whether the block can be modulated by cycling of the channel through different states, similar to the use-dependent block of sodium channels by local anesthetics (66), remains to be explored.

We express our appreciation to Dr. Enrico Stefani and Garland Cantrell for design and construction of the bilayer amplifier; to Dr. Michael Fill for helpful advice, encouragement, and numerous discussions concerning this study; to Dr. Ivan Zahradník for valuable comments and suggestions during manuscript preparation; to Monte Crawford for assistance with animal handling; to Christine Dettbarn for assistance with some of the microsomal preparations and for protein determinations; and to the Baylor College of Medicine, Department of Medicine, Section of Cardiovascular Sciences for the loan of a Polytron homogenizer.

This work was supported by Department of Health and Human Services PO1 HL37044 and RO1 HL 42527 and American Heart Association 881112.

Note added in proof: Tinker and Williams (1993. *Biophys. J.* 64:A302) and Xu, Jones, and Meissner (1993. *J. Gen. Physiol.*, 101:207–233)have recently reported open channel block of the SR Ca release channel by positively charged local anesthetics at positive potentials.

Received for publication 26 February 1992 and in final form 14 December 1992.

REFERENCES

1. Ashley, R. H., and A. J. Williams. 1990. Divalent cation activation and inhibition of single calcium release channels from sheep cardiac sarcoplasmic reticulum. *J. Gen. Physiol.* 95:981–1005.

2. Smith, J. S., T. Imagawa, J. Ma, M. Fill, K. P. Campbell, and R. Coronado. 1988. Purified ryanodine receptor from rabbit skeletal muscle is the calcium-release channel of sarcoplasmic reticulum. *J. Gen. Physiol.* 92:1–26.
3. Block, B. A., T. Imagawa, K. P. Campbell, and C. Franzini-Armstrong. 1988. Structural evidence for direct interaction between the molecular components of the transverse tubule/sarcoplasmic reticulum junction in skeletal muscle. *J. Cell Biol.* 107:2587–2600.
4. Baylor, S. M., S. Hollingworth, and M. W. Marshall. 1989. Effects of intracellular ruthenium red on excitation-contraction coupling in intact frog skeletal muscle fibres. *J. Physiol. (Lond.).* 408:617–635.
5. Palade, P., D. Brunder, C. Dettbarn, and P. Stein. 1990. A pharmacologic approach to the physiological mechanism of excitation-contraction coupling. *In* Transduction in Biological Systems. J. Bacigualpo, C. Hidalgo, E. Jaimovich, C. Vergara, and J. Vergara, editors. Plenum Press, New York. 401–414.
6. Brunder, D. G., S. Gyorke, C. Dettbarn, and P. Palade. 1992. Involvement of sarcoplasmic reticulum 'Ca^{2+} release channels' in excitation-contraction coupling in vertebrate skeletal muscle. *J. Physiol. (Lond.).* 445:759–778.
7. Smith, J. S., R. Coronado, and G. Meissner. 1986. Single channel measurements of the calcium release channel from skeletal muscle sarcoplasmic reticulum. *J. Gen. Physiol.* 88:573–588.
8. Bull, R., J. J. Marengo, B. A. Suarez-Isla, P. Donoso, J. L. Sutko, and C. Hidalgo. 1989. Activation of calcium channels in sarcoplasmic reticulum from frog muscle by nanomolar concentrations of ryanodine. *Biophys. J.* 56:749–756.
9. Kawasaki, T., and M. Kasai. 1989. Disulfonic stilbene derivatives open the Ca^{2+} release channel of sarcoplasmic reticulum. *J. Biochem. (Tokyo).* 106:401–405.
10. Rousseau, E., and G. Meissner. 1989. Single cardiac sarcoplasmic reticulum Ca^{2+}-release channel: activation by caffeine. *Am. J. Physiol.* 256:H328–H333.
11. Ondriáš, K., L. Borgatta, D. H. Kim, and B. E. Ehrlich. 1990. Biphasic effects of doxorubicin on the calcium release channel from sarcoplasmic reticulum of cardiac muscle. *Circ. Res.* 67:1167–1174.
12. Holmberg, S. R. M., and A. J. Williams. 1990. The cardiac sarcoplasmic reticulum calcium-release channel: modulation of ryanodine binding and single-channel activity. *Biochim. Biophys. Acta.* 1022:187–193.
13. Sitsapesan, R., and A. J. Williams. 1990. Mechanisms of caffeine activation of single calcium release channels of sheep cardiac reticulum. *J. Physiol. (Lond.).* 423:425–439.
14. Williams, A. J., and S. R. M. Holmberg. 1990. Sulmazole (AR-L 115BS) activates the sheep cardiac muscle sarcoplasmic reticulum calcium-release channel in the presence and absence of calcium. *J. Membr. Biol.* 115:167–178.
15. Valdivia, H. H., C. Valdivia, J. Ma, and R. Coronado. 1990. Direct binding of verapamil to the ryanodine receptor channel of sarcoplasmic reticulum. *Biophys. J.* 58:471–481.
16. Rousseau, E., J. S. Smith, J. S. Henderson, and G. Meissner. 1986. Single channel and $^{45}Ca^{2+}$ flux measurements of the cardiac sarcoplasmic reticulum calcium channel. *Biophys. J.* 50:1009–1014.
17. Ma, J., M. Fill, C. M. Knudson, K. P. Campbell, and R. Coronado. 1988. Ryanodine receptor of skeletal muscle is a gap junction-type channel. *Science (Wash. DC).* 242:99–102.
18. Anderson, K., F. A. Lai, Q.-Y. Liu, E. Rousseau, H. P. Erickson, and G. Meissner. 1989. Structural and functional characterization of the purified cardiac ryanodine receptor–Ca^{2+} release channel complex. *J. Biol. Chem.* 264:1329–1335.
19. Hille, B. 1977. Local anesthetics: hydrophilic and hydrophobic pathways for the drug-receptor reaction. *J. Gen. Physiol.* 69:497–515.
20. Hondeghem, L. M., and B. G. Katzung. 1977. Time- and voltage-dependent interactions of antiarrhythmic drugs with cardiac sodium channels. *Biochim. Biophys. Acta.* 472:373–398.
21. Feinstein, M. B. 1963. Inhibition of caffeine rigor and radiocalcium movements by local anesthetics in frog sartorius muscle. *J. Gen. Physiol.* 47:151–171.
22. Antoniu, B., D. H. Kim, H. Morii, and N. Ikemoto. 1985. Inhibitors of Ca^{2+} release from the sarcoplasmic reticulum. *Biochim. Biophys. Acta.* 816:9–17.
23. Bianchi, C. P., and T. C. Bolton. 1967. Action of local anesthetics on coupling systems in muscle. *J. Pharmacol. Exp. Ther.* 157:388–405.
24. Heistracher, P., and C. C. Hunt. 1969. The effect of procaine on snake twitch muscle fibres. *J. Physiol. (Lond.).* 201:627–638.
25. Klein, M. G., B. J. Simon, and M. F. Schneider. 1992. Effects of procaine and caffeine on calcium release from the sarcoplasmic reticulum in frog skeletal muscle. *J. Physiol. (Lond.).* 453:341–366.
26. Uhrík, B., and D. Zacharová. 1976. Recovery of ultrastructural changes accompanying caffeine contractures in isolated muscle fibres of the crayfish. *Pfluegers Arch.* 364:183–190.
27. Györke, S., and P. Palade. 1992. Calcium-induced calcium release in crayfish skeletal muscle. *J. Physiol. (Lond.).* 457:195–210.
28. Endo, M., and S. Thorens. 1975. Mechanism of release of calcium from the sarcoplasmic reticulum. *In* Calcium Transport in Contraction and Secretion. E. Carafoli, F. Clementi, W. Drabikowski, and A. Margreth, editors. North-Holland Publ. Co., Amsterdam. 359–366.
29. Donaldson, S. K. B. 1985. Peeled mammalian skeletal muscle fibers. Possible stimulation of Ca^{2+} release via a transverse tubule-sarcoplasmic reticulum mechanism. *J. Gen. Physiol.* 86:501–525.
30. Weber, A., and R. Herz. 1968. The relationship between caffeine contracture of intact muscle and the effect of caffeine on reticulum. *J. Gen. Physiol.* 52:750–759.
31. Thorpe, W. R., and P. Seeman. 1971. The site of action of caffeine and procaine in skeletal muscle. *J. Pharmacol. Exp. Ther.* 179:324–330.
32. Nagasaki, K., and M. Kasai. 1981. Calcium-induced calcium release from sarcoplasmic reticulum vesicles. *J. Biochem. (Tokyo).* 90:749–755.
33. Chapman, R. A., and D. J. Miller. 1974. The effects of caffeine on the contraction of the frog heart. *J. Physiol. (Lond.).* 242:589–613.
34. Chamberlain, B. K., P. Volpe, and S. Fleischer. 1984. Inhibition of calcium-induced calcium release from purified cardiac sarcoplasmic reticulum vesicles. *J. Biol. Chem.* 259:7547–7553.
35. Ooshima, N., K. Horiuti, T. Kitazawa, and M. Endo. 1985. Dual effects of procaine on caffeine contracture of cardiac muscle. *Jpn. J. Pharmacol.* 39:139P.
36. Stephenson, D. G., and I. R. Wendt. 1986. Effects of procaine on calcium accumulation by the sarcoplasmic reticulum of mechanically disrupted rat cardiac muscle. *J. Physiol. (Lond.).* 373:195–207.
37. Smith, J. S., R. Coronado, and G. Meissner. 1985. Sarcoplasmic reticulum contains adenine nucleotide-activated calcium channels. *Nature (Lond.).* 316:446–449.
38. Rardon, D. P., D. C. Cefali, R. D. Mitchell, S. M. Seiler, and L. R. Jones. 1989. High molecular weight proteins purified from cardiac junctional sarcoplasmic reticulum vesicles are ryanodine-sensitive calcium channels. *Circ. Res.* 64:779–789.
39. Zimányi, I., and I. N. Pessah. 1991. Comparison of [^{3}H]ryanodine

receptors and Ca^{++} release from rat cardiac and rabbit skeletal muscle sarcoplasmic reticulum. *J. Pharmacol. Exp. Ther.* 256:938–946.

40. Harigaya, S., and A. Schwartz. 1969. Rate of calcium binding and uptake in normal animal and failing human cardiac muscle. *Circ. Res.* 25:781–794.
41. Fabiato, A., and F. Fabiato. 1979. Calculator programs for computing the composition of the solutions containing multiple metals and ligands used for experiments in skinned muscle cells. *J. Physiol. (Paris).* 75:463–505.
42. Hamilton, S. L., R. Mejia Alvarez, M. Fill, M. J. Hawkes, K. L. Brush, W. P. Schilling, and E. Stefani. 1989. [3H]PN200-110 and [3H]ryanodine binding and reconstitution of ion channel activity with skeletal muscle membranes. *Analyt. Biochem.* 183:31–41.
43. Colquhoun, D., and F. J. Sigworth. 1983. Fitting and statistical analysis of single channel records. *In* Single Channel Recording. B. Sakmann and E. Neher, editors. Plenum Press, New York. 191–263.
44. Chu, A., M. Fill, M. L. Entman, and E. Stefani. 1991. Different Ca^{2+} sensitivity of the ryanodine-sensitive Ca^{2+} release channels of cardiac and skeletal muscle sarcoplasmic reticulum. *Biophys. J.* 59:102a.
45. Colquhoun, D., and A. G. Hawkes. 1983. The principles of the stochastic interpretation of ion channel mechanisms. *In* Single Channel Recording. B. Sakmann and E. Neher, editors. Plenum Press, New York. 135–175.
46. Chay, T. R. 1988. Kinetic modeling for the channel gating process from single channel patch clamp data. *J. Theor. Biol.* 132:449–468.
47. Fill, M., R. Coronado, J. R. Mickelson, J. Vilven, J. Ma, B. A. Jacobson, and C. F. Louis. 1990. Abnormal ryanodine receptor channels in malignant hyperthermia. *Biophys. J.* 57:471–475.
48. Kawano, S., and R. L. DeHaan. 1991. Developmental changes in the calcium currents in embryonic chick ventricular myocytes. *J. Membr. Biol.* 120:17–28.
49. Coronado, R., and J. S. Smith. 1987. Monovalent ion current through single calcium channels of skeletal muscle transverse tubules. *Biophys. J.* 51:497–502.
50. Hess, P., J. B. Lansman, and R. W. Tsien. 1986. Calcium channel selectivity for divalent and monovalent cations. Voltage and concentration dependence of single channel current in ventricular heart cells. *J. Gen. Physiol.* 88:293–319.
51. Levi, R., and L. J. DeFelice. 1986. Sodium-conducting channels in cardiac membranes in low calcium. *Biophys. J.* 50:5–9.
52. Kawano, S., and R. L. DeHaan. 1990. Analysis of the T-type calcium channel in embryonic chick ventricular myocytes. *J. Membr. Biol.* 116:9–17.
53. Almers, W., E. W. McCleskey, and P. T. Palade. 1984. A non-selective cation conductance in frog muscle membrane blocked by micromolar external calcium ions. *J. Physiol. (Lond.).* 353:565–583.
54. Hess, P., and R. W. Tsien. 1984. Mechanism of ion permeation through calcium channels. *Nature (Lond.).* 309:453–456.
55. Lansman, J. B., P. Hess, and R. W. Tsien. 1986. Blockade of current through single calcium channels by Cd^{2+}, Mg^{2+}, and Ca^{2+}. Voltage and concentration dependence of calcium entry into the pore. *J. Gen. Physiol.* 88:321–347.
56. Colombini, M. 1979. A candidate for the permeability pathway of the outer mitochondrial membrane. *Nature (Lond.).* 279:643–645.
57. Lindsay, A. R. G., S. D. Manning, and A. J. Williams. 1991. Monovalent cation conductance in the ryanodine receptor-channel of sheep cardiac muscle sarcoplasmic reticulum. *J. Physiol. (Lond.).* 439:463–480.
58. McLaughlin, S., and M. Whitaker. 1988. Cations that alter surface potentials of lipid bilayers increase the calcium requirement for exocytosis in sea urchin eggs. *J. Physiol. (Lond.).* 396:189–204.
59. Young, H. S., V. Skita, R. P. Mason, and L. G. Herbette. 1992. Molecular basis for the inhibition of 1,4-dihydropyridine calcium channel drugs binding to their receptors by a nonspecific site interaction mechanism. *Biophys. J.* 61:1244–1255.
60. Endo, M. 1981. Mechanism of calcium-induced calcium release in the SR membrane. *In* The Mechanism of Gated Calcium Transport across Biological Membranes. S. T. Ohnishi and M. Endo, editors. Academic Press, New York. 257–264.
61. Pike, G. K., J. J. Abramson, and G. Salama. 1989. Effects of tetracaine and procaine on skinned muscle fibres depend on free calcium. *J. Muscle Res. Cell Motil.* 10:337–349.
62. Bianchi, C. P. 1968. Pharmacological actions on excitation-contraction coupling in striated muscle. *Fed. Proc.* 27:126–131.
63. Neher, E., and J. H. Steinbach. 1978. Local anaesthetics transiently block currents through single acetylcholine receptor channels. *J. Physiol. (Lond.).* 277:153–176.
64. Rosenberg, R. L., P. Hess, and R. W. Tsien. 1988. Cardiac calcium channels in planar lipid bilayers. L-type channels and calcium permeable channels open at negative membrane potentials. *J. Gen. Physiol.* 92:27–54.
65. Moczydlowski, E., A. Uehara, and S. Hall. 1986. Blocking pharmacology of batrachotoxin-activated sodium channels. *In* Ion Channel Reconstitution. C. Miller, editor. Plenum Press, New York. 405–428.
66. Courtney, K. R. 1975. Mechanism of frequency-dependent inhibition of sodium currents in frog myelinated nerve by the lidocaine derivative GEA 968. *J. Pharmacol. Exp. Ther.* 195:225–236.
67. Magleby, K. L., and B. S. Pallotta. 1983. Burst kinetics of single calcium-activated potassium channels in cultured rat muscle. *J. Physiol. (Lond.).* 344:605–623.